- Technical Paper -

A STUDY ON RESIDUAL CAPACITY OF REINFORCED CONCRETE CORBEL FAILED BY ANCHORAGE SPLITTING FAILURE

Liyanto EDDY[*1], Kohei NAGAI[2], and Ram Chandra NEUPANE[3]

ABSTRACT

Some bearing pads were installed at the free end of the corbel and an anchorage splitting failure occurs. However, if the bearing pad is moved to the straight portion of the flexural reinforcements of the corbel, there is a possibility that the corbel is still able to resist the load, which is called residual capacity. In this study, the residual capacity of a reinforced concrete corbel, failed by an anchorage splitting failure, is investigated, both by experimental work and numerical simulation. By the simulation, using RBSM, different crack failure patterns can be simulated due to different positions of bearing pads. Eventually, the residual capacity of the corbel failed by the anchorage splitting failure is still very large. The option to move the bearing pad to the straight portion of the flexural reinforcements of the corbel can be a simple way for recovering the capacity of a corbel failed by the local failure.

Keywords: corbel, residual capacity, anchorage splitting failure, Rigid Body Spring Model

1. INTRODUCTION

Corbel is a short cantilever member that comes out from a column, a wall, or a bridge pier, to sustain a load, originating from a gantry girder or a precast concrete beam. A corbel is generally built monolithically with a column or a wall, and is characterized by a low shear span-to-depth ratio. To transfer a load from a beam to a corbel, a bearing pad is usually installed on the corbel. However, for the easiness of the construction, some bearing pads were installed in the wrong position, at the free end of corbels. The position of the bearing does not satisfy the requirement in the design code [1].

Generally, the failure of a corbel can be divided into several typical modes [2]. When a load is applied too near the free end of a short cantilever, an anchorage splitting failure along the anchored flexural reinforcement can occur (Fig.1). Meanwhile, few cracks, either diagonal compression cracks or flexural cracks, occur in the corbel. Based on this behavior, if the location of bearing pad is moved to the straight portion of the flexural reinforcement of the corbel, there is still a possibility that the corbel is still able to resist the load, although a local failure occurs. Furthermore, the option to move the bearing pad to the straight portion of the flexural reinforcement might be a simple way for recovering the capacity of a corbel failed by the anchorage splitting failure. However, how much load that a corbel is still able to resist after a local failure occurs, which is called residual capacity, has not been investigated.

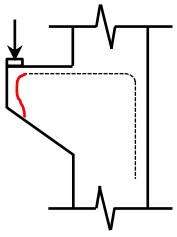

Fig.1 Anchorage splitting failure of a corbel

In order to study the residual capacity of a reinforced concrete corbel failed by an anchorage splitting failure, there are 2 alternatives, i.e. experimental works and computational numerical simulations. Through experimental works, the real load-displacement relationship and surface cracks can be obtained easily. However, the internal cracks and the internal stress are difficult to be observed. Our research group has conducted a meso-scale analysis of reinforced concrete members by a 3-dimensional discrete element analysis, called RBSM. The study on a reinforced concrete member at the meso-scale, in which the local re-bar arrangement is considered by modeling the rib of re-bar, is useful for the precise evaluation of its behavior, since at this level, cracks occur as the result of the interlock mechanism between concrete and re-bar. Moreover, Ikuta *et al.* [3] successfully simulated different crack patterns with different bending radius of re-bars of L-shaped beam column joint with simple arrangement of re-bars by RBSM. Meanwhile, the residual capacity analysis of a reinforced concrete member has not been introduced in RBSM. Eventually, the purpose of this study is to study the residual

*1 Graduate Student, Department of Civil Engineering, The University of Tokyo, Tokyo, Japan, JCI Student Member. Email: eddy@iis.u-tokyo.ac.jp
*2 Associate Professor, International Center for Urban Safety Engineering, Institute of Industrial Science, The University of Tokyo, Tokyo, Japan, JCI Member
*3 Graduate Student, Department of Civil Engineering, The University of Tokyo, Tokyo, Japan, JCI Member

capacity of a reinforced concrete corbel failed by an anchorage splitting failure, both by experimental work and numerical simulation.

2. TEST PROGRAMS

2.1 Experimental Specimens

To study the residual capacity of a corbel failed by an anchorage splitting failure, 3 reinforced concrete corbels were loaded with different loading positions (see Table 1). The specimens were reinforced with reinforcing bars. The column segment was reinforced by four longitudinal deformed bars of 16 mm and six lateral ties of 10 mm. Deformed bars of 13 mm, that were used as the flexural reinforcements of the corbel, were bent through 90 degree. Two deformed bars of 10 mm were used as the lateral ties of the corbel. The distance between the top surface of the concrete and the top surface of the outer stirrups, of all specimens is 20 mm. Fig.2 shows the dimension and the reinforcing bars arrangement of the experimental specimens.

For the recognition of the variable in each model, the following notations were used. EC signifies the specimen with bearing pads installed and loaded on the edge of the corbel. The purpose of Corbel EC is to verify the occurrence of anchorage splitting cracks. MC signifies the specimen with bearing pads installed and loaded on the straight portion of the flexural reinforcement of the corbel. Corbel MC is intended as the control specimen. RCC signifies the specimen for investigating the residual capacity of a corbel. To study the residual capacity of the corbel, Corbel EC, after being failed by the anchorage splitting failure, was re-used as Corbel RCC. Before the specimen was re-loaded on the straight portion of flexural reinforcements of the corbel, the specimen was un-loaded.

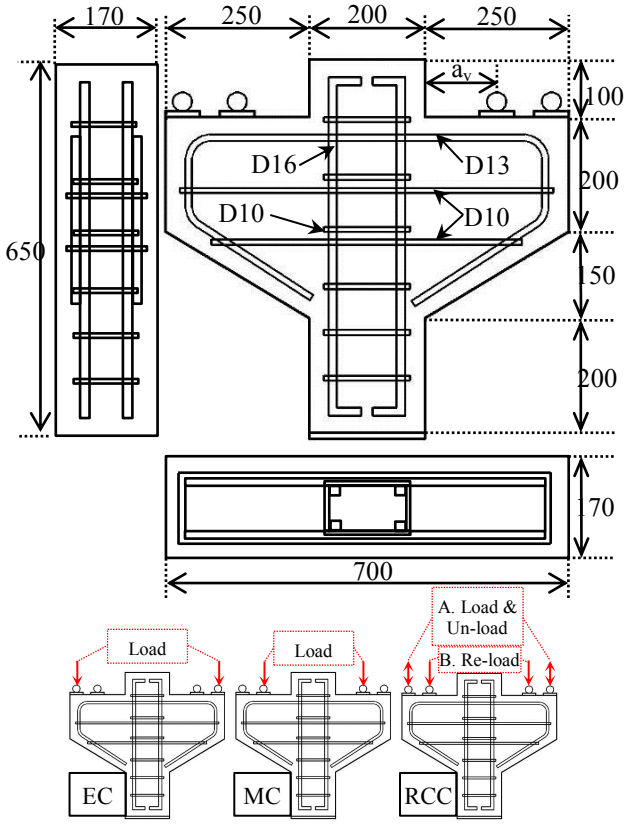

Fig.2 Dimension and re-bars arrangement of experimental specimens (Units: mm)

2.2 Materials

(1) Concrete

A concrete compressive strength of 40 MPa was used for mix design, using maximum 20 mm of coarse aggregate size. Standard compressive cylinder tests and standard split cylinder tests were conducted to determine the values of the compressive strength and the splitting tensile strength of the concrete, respectively. The compressive strengths and the splitting tensile strengths of the concrete specimens are listed in Table 1.

(2) Reinforcing Materials

Deformed bars of 16 mm, 13 mm, and 10 mm were used. The yield strengths of deformed bars of 16 mm and 13 mm are same in both diameters, i.e. 490MPa and the yield strength of deformed bars of 10 mm is 390 MPa.

2.3 Test Setup and Measurements

The corbels were loaded on the column segment in an upside-down position using a Universal Test Machine (UTM). Meanwhile, the corbels were seated on steel roller supports at different positions, depending on the position of the bearing pads. Thin layer of gypsum was used between the bearing plates and the specimen to ensure the stability during loading. Load was applied at a constant rate of 0.0084 mm per second. At each step of load, the total load was measured by using a load cell and relative displacements of bearing pads were measured by using Linear Voltage Differential Transducers (LVDTs). Fig.3 shows the detail of the test setup.

3. ANALYSIS METHOD

In this study, the simulation is carried out by

Table.1 Detail of experimental specimens

Case	Parameter	Shear Span	Reinforcing Bars				Strength of Concrete	
			Column		Corbel		Compression	Tension
		a_v (mm)	Longitudinal	Transverse	Longitudinal	Transverse	$f'c$ (Mpa)	f_t (Mpa)
EC	Loading on Edge Pad	125	4-D16	6-D10	2-D13	2-D10	45.52	2.66
MC	Loading on Middle Pad	220	4-D16	6-D10	2-D13	2-D10	41.89	2.81
RCC	Residual Capacity	220	4-D16	6-D10	2-D13	2-D10	45.52	2.66

Table.2 Detail of numerical models

Case	Parameter	Shear	Strength of Concrete		Number of	Maximum Load	
			Compression	Tension	Element	EXP	ANA
		a_v (mm)	$f'c$ (Mpa)	f_t (Mpa)		(kN)	(kN)
EC	Loading on Edge Pad	125	45.52	2.66	318494	428	354
MC	Loading on Middle Pad	220	41.89	2.81	318448	229	199
RCC	Residual Capacity	220	45.52	2.66	318747	409	301

Fig.3 Test setup

3-dimensional RBSM, proposed by Kawai *et al.* [4]. In RBSM, a 3 dimensional reinforced concrete model is meshed into rigid bodies. Each rigid body consists of 6 degree of freedoms, i.e. 3 translational degrees of freedom and 3 rotational degrees of freedom at some points within its interior and connects with other rigid bodies by 3 springs, i.e. 2 shear springs and 1 normal spring. As the propagation of cracks in reinforced concrete is one of the most important factors in investigating the behavior of reinforced concrete members, the mesh arrangement of the model in RBSM is important. In order to prevent cracks propagated in a non-arbitrary direction, a random geometry, called Voronoi Diagram, is used for the element meshing. The concrete element size is modeled approximately 1-2 cm^3 that is similar to the aggregate size. The geometry of steel elements is modeled in an accurate manner, by modeling a 3-dimensional arrangement of reinforcing bar, to properly account for the interlock between the reinforcing bar and concrete. Mesh arrangement of concrete and steel at meso-scale in this study is shown in Fig.4. To model a 3-dimensional reinforced concrete member, two types of elements are used, i.e. concrete element and steel element. The properties of the springs are determined so that the elements, when combined together, enable to predict the behaviour of the model as accurate as that of the experimental result. In this study, the simulation system, developed by Nagai *et al.* [5], is used and the constitutive models of the elements are adopted from Ikuta *et al.* [3]. Fig.5 shows the constitutive model of the concrete element.

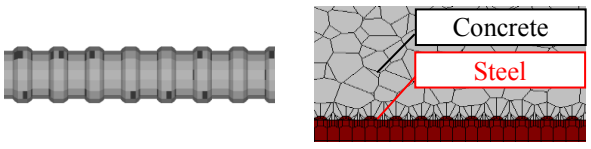

(a) Model of 3D Re-bar (b) Cross section

Fig.4 Mesh arrangement of concrete and re-bar

4. DETAILS OF NUMERICAL SIMULATIONS

4.1 Numerical Model

Table.2 shows the numerical models that were conducted in order to study the residual capacity of a corbel failed by an anchorage splitting failure. The same notations with experiment specimens were used. 3 numerical models, with different positions of bearing pads, were modeled.

4.2 Geometry of Numerical Model

The same dimensions, as experimental specimens, were modeled. However, for the simplification of the models and in order to reduce the computational time, only one side of the corbels was modeled and the stirrups in the column segment were not modeled. Fig.6. shows the geometry of the numerical models.

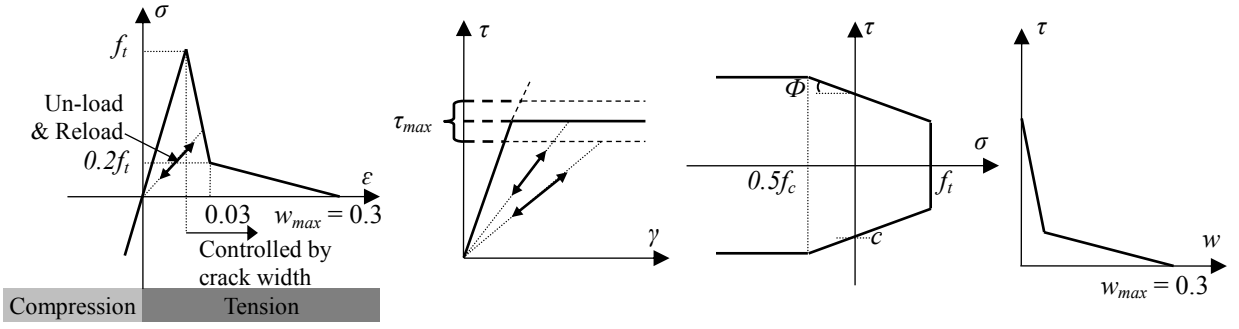

(a) Normal spring (b) Shear spring (c) Failure criterion (d) Shear reduction

Fig.5 Constitutive model of concrete

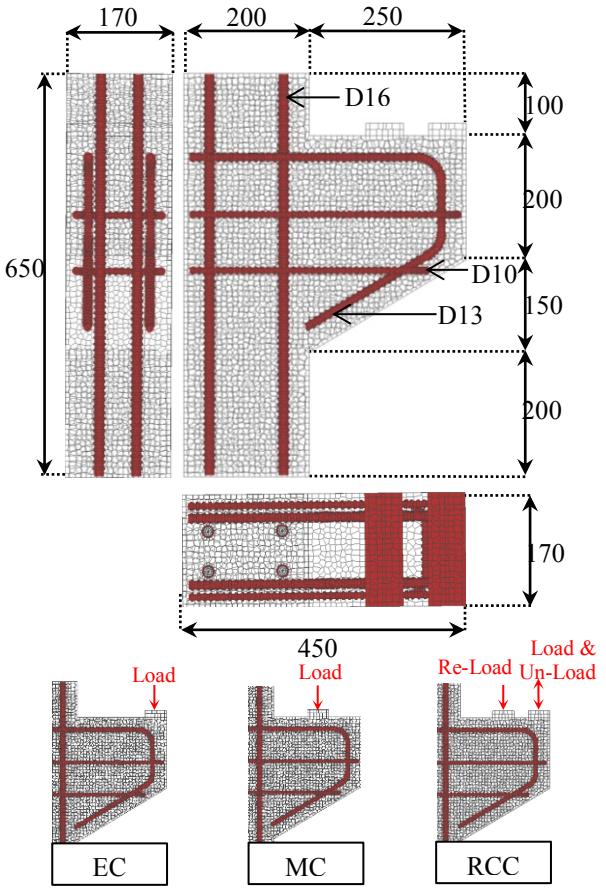

Fig.6 Geometry of numerical models (Units: mm)

4.3 Boundary Condition

Fig.7 shows the boundary conditions of numerical models. Fix condition in all direction is assumed at the top and the bottom of the column segment. Monotonically displacement-load controlled was applied on the bearing pad of the corbel. The displacement-load increases 0.016 mm for every step of load. 200 steps of displacement-load were applied in the simulation. The boundary condition in the column segment is different with the experimental test setup. However, it has been confirmed that this boundary condition does not affect the simulation results, i.e. load-displacement relationships and crack patterns.

In order to introduce the residual capacity

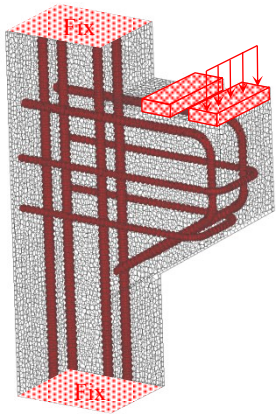

Fig.7 Boundary Condition

analysis in the numerical simulation of Corbel RCC, 2 bearing pads were modeled in case of corbel RCC, i.e. an edge bearing pad and a middle bearing pad. The same load pattern with experiment was applied. As the initial load, the load was applied on the edge bearing pad. After the load reached the maximum load, the load was un-loaded until the force was zero. After the un-loaded process was completed, the loading position was moved and applied on the middle bearing pad.

5. RESULTS AND DISCUSSIONS

5.1 Load-Displacement Relationships

Fig.8 and Fig.9 show the load-displacement relationships of experimental specimens and numerical models, respectively. Table.2 shows the maximum loads of experimental specimens and numerical models. The load of load-displacement relationships of experimental specimens was calculated based on the total load which was measured by a load cell. The displacement of load-displacement relationships of experimental specimens was determined based on the average relative displacement, which was measured by LVDTs. Experimental results are shown until the peak load because the measurements were not stable in the post peak due to the brittle failure. Meanwhile, the load and the displacement of the load-displacement relationships of the numerical models were determined based on the load and the displacement which were applied on the bearing pad.

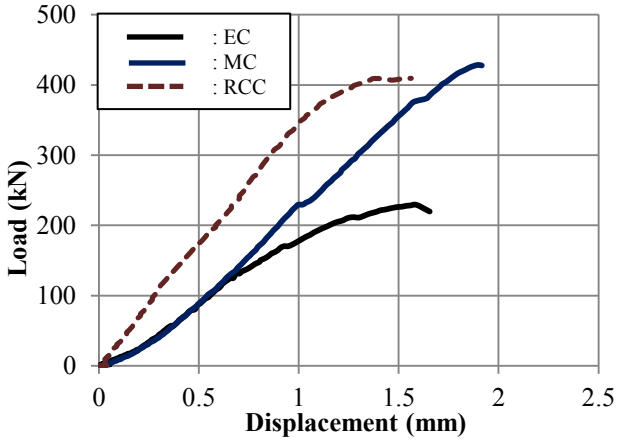

Fig.8 Load-displacement relationships of experimental specimens

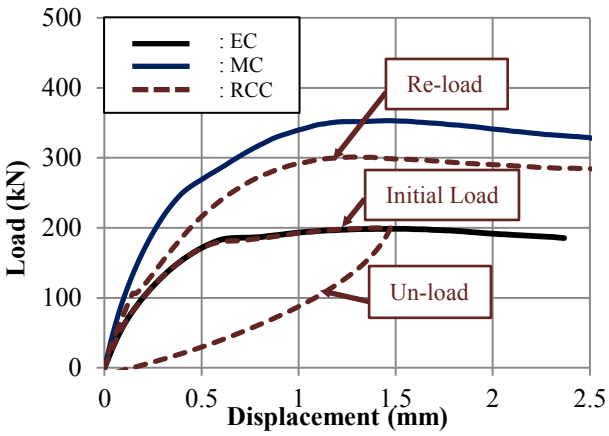

Fig.9 Load-displacement relationships of numerical results

The maximum loads of the numerical models are roughly the same as those of experimental specimens, i.e. approximately 13-17% difference. In case of corbel EC, the simulation prediction is underestimate by 13%, and in case of corbel MC, the simulation prediction is underestimate by 17%. The initial stiffness of the experimental results is lower than that of simulation results. Crushing gypsum layer, located between the bearing pad and the corbel, might cause the lower initial stiffness of the experimental results.

Both experimental and numerical results show that the maximum load of corbel EC is reduced by approximately 45 % of reduction ratio compared with that of corbel MC. It can be concluded that the position of the bearing pad is important. When the load is applied on the edge of the corbel, the load capacity of the corbel will be reduced significantly.

In case of corbel RCC, both experimental and numerical results show that the maximum load of corbel RCC is higher than that of corbel EC. The results show that the capacity of a corbel can be recovered when the loading position is moved to the straight portion of the flexural reinforcements of the corbel. Although the capacity of the corbel cannot be fully recovered, both experimental and numerical results show that the residual capacity of the corbel is still very large, i.e. 95% by experimental observation and 85% by numerical prediction. Initial damage may cause that the capacity of the corbel could not be fully recovered. Furthermore, the option to move the bearing pad to the straight portion of the flexural reinforcements can be a simple way for recovering the capacity of a corbel failed by an anchorage splitting failure. However, the site condition should be considered whether the position of the bearing pad can be moved.

5.2 Internal Cracks of Simulation Results

Fig.10, Fig.11, and Fig.12 show the internal cracks of corbel EC, corbel MC, and corbel RCC respectively. Yellow color, orange color, and red color indicate the crack face with crack width of 0.03 mm, 0.1 mm, and 0.3 mm, respectively. Generally, the crack propagations of the numerical models are roughly the same as those of the experimental specimens.

In case of corbel EC, when the load is relatively small, flexural cracks occur at the corbel-column interface (Fig.10.a). As the load increases, diagonal cracks occur, propagating from the position of the bearing pad to the sloping end of the corbel (Fig.10.b). In addition, simulation result can provide more detail information how the anchorage splitting cracks occur. In the early stage of the formation of the anchorage splitting cracks, cracks occur along the bending portion of the flexural reinforcements of the corbel (Fig.10.c). As the result, the stiffness of the load-displacement relationship is reduced dramatically. As the load increases, cracks propagate along the anchorage (Fig.10.d and Fig.10.e).

In case of corbel MC, when the load is relatively small, flexural cracks occur at the corbel-column interface (Fig.11.a). As the load increases, diagonal cracks, propagating from the position of the bearing pad to the sloping end of the corbel (Fig.11.b). When the load reaches the maximum load, no other type of cracks occurs in the corbel, beside the flexural cracks and diagonal cracks (Fig.11.c). Based on the simulation results, cracks occur in the column segment as the result of the simplification of the models, i.e. no stirrup of column was modeled.

In case of corbel RCC, when the load of the corbel is un-loaded, the process of the closing of cracks can be simulated well (Fig.12.a, Fig.12.b, and Fig.12.c). When the loading position is moved and re-loaded on the middle bearing pad, new diagonal cracks occur in the corbel, propagating from the position of the new bearing pad to the sloping end of the corbel.

5.3 Crack Patterns at Failure

Fig.13, Fig.14, and Fig. 15 show the crack patterns of the experimental specimens, compared with

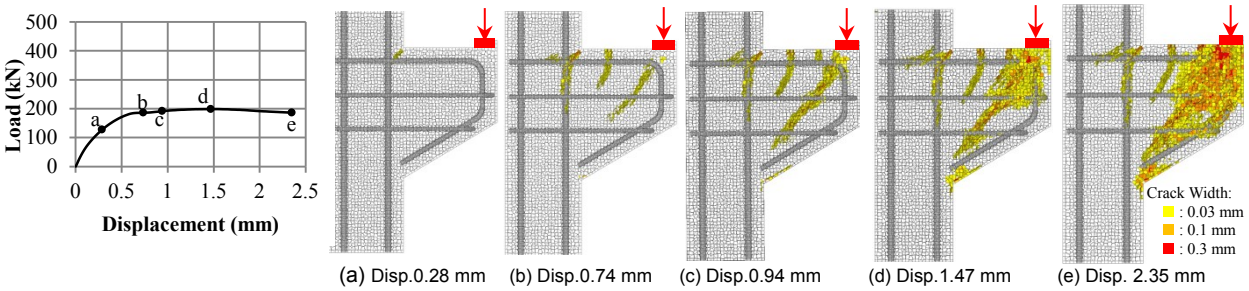

Fig.10 Internal cracks of numerical model of corbel EC

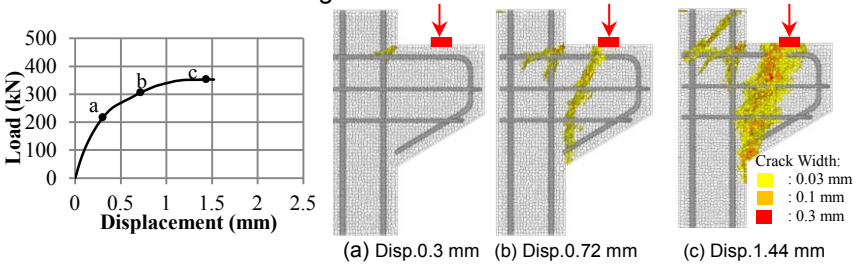

Fig.11 Internal cracks of numerical model of corbel MC

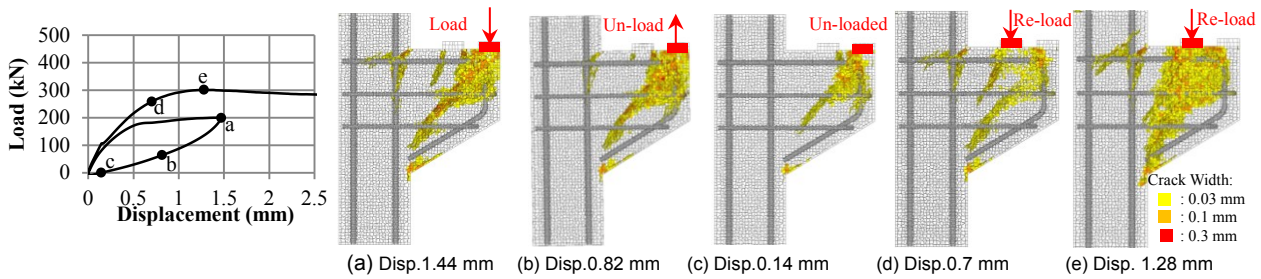

Fig.12 Internal cracks of numerical model of corbel RCC

the numerical models at failure. The displacement of the models is enlarged by 10 times. Simulation results can predict the crack patterns at failure as well as those of experimental results.

Based on the crack pattern of corbel EC, flexural cracks, anchorage splitting cracks, and diagonal cracks propagating from the position of the bearing pad to the sloping end of the corbel occur in the numerical models and experimental specimens. In case of corbel MC, flexural cracks and diagonal cracks, propagating from the position of the bearing pad to the sloping end of the corbel occur in both numerical models and experimental specimens. Furthermore, flexural cracks, anchorage splitting cracks, anchorage splitting cracks, previous and new diagonal cracks occur in both numerical models and experimental specimens in case of corbel RCC.

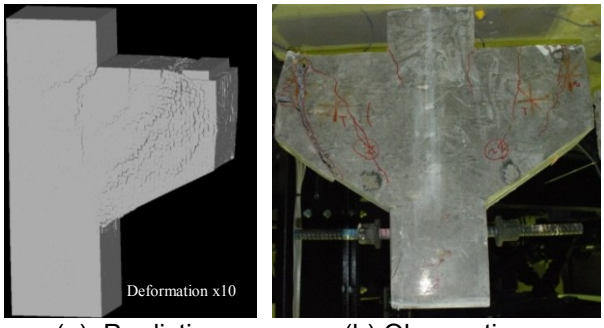

(a) Prediction (b) Observation

Fig.13 Failure pattern of corbel EC

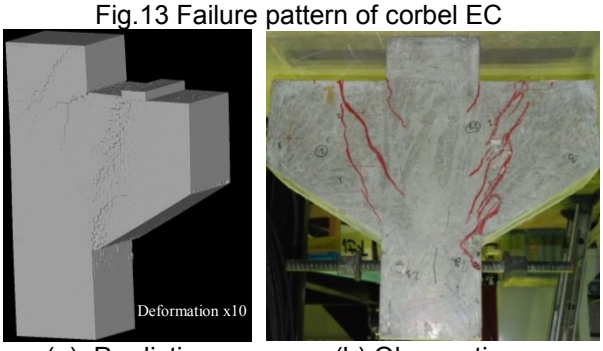

(a) Prediction (b) Observation

Fig.14 Failure pattern of corbel MC

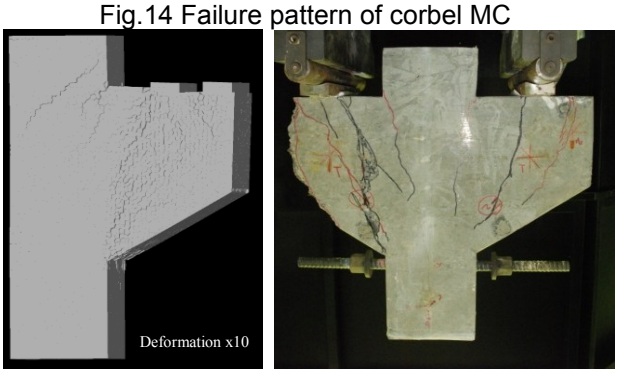

(a) Prediction (b) Observation

Fig.15 Failure pattern of corbel RCC

6. CONCLUSIONS

(1) Based on the experimental results, the capacity of the corbel is reduced by approximately 45% of reduction ratio when the load is applied on the edge of the corbel. On the other hand, when a corbel failed by an anchorage splitting failure is re-loaded on the straight portion on the flexural reinforcements of the corbel, the corbel is still able to resist the load. It was observed that the residual capacity of the corbel is still very large, i.e. 95%. The option to move the bearing pad to the straight portion of flexural reinforcements of the corbel can be a simple way for recovering the capacity of a corbel failed by the local failure. However, the condition in construction site should be considered in practice.

(2) Different failure pattern can be simulated due to different position of bearing pad by RBSM. The analysis could explain well the failure mechanism due to different position of bearing pad.

REFERENCES

[1] Subcommittee on English Version of Standard Specifications for Concrete Structures, "Standard Specification for Concrete Structures "Design"," Japan Society of Civil Engineers (JSCE), December 2010.

[2] Kriz, L. B., Raths, C.H., "Connections in Precast Concrete Institute-Strength of Corbels," Journal of Prestressed Concrete Institute, Vol.10, No.1, February 1965, p.p. 16-61.

[3] Ikuta, K.; Nagai, K.; Hayashi, D., "Numerical Simulation of Beam-Column Join with Simple Reinforcement Arrangement by Three-dimensional RBSM," International Symposium of New Technologies for Urban Safety Mega Cities in Asia (USMCA), 2012.

[4] Kawai, T., "New Discrete Models and Their Application to Seismic Response Analysis of Structure," Nuclear Engineering and Design, 48, 207-229. 1978.

[5] Nagai, K.; Sato, Y.; Ueda, T., "Mesoscopic Simulation of Failure of Mortar and Concrete by 2D RBSM," J. Adv. Conc. Technol., 3(3), 385-402. 2005.